SPE Plastics Research Online
SOCIETY OF PLASTICS ENGINEERS
10.2417/spepro.006369

Predicting flow-induced stress during injection/compression molding

Wei Cao, Qian Zhang, Yanhui Qi, Guixiang Lu, and Changyu Shen

A new approach, which combines the eXtended Pom-Pom finite element model and an arbitrary Lagrangian-Eulerian technique, is used to simulate stress levels at different points in a molded part.

During the compression stage of injection/compression molding (ICM) processes, an evenly distributed external force is exerted on the melt, which allows molecular orientation to be minimized and flow-induced stresses to be reduced.[?] These flow-induced stresses are complex because the compression flow combines aspects of both shear and extensional flow. The residual flow-induced stresses are also responsible for the anisotropy of the produced part's mechanical, thermal, and optical properties. Furthermore, the stresses affect the long-term dimensional stability of the part. However, few tools or software are currently available—because of a lack of sound theoretical studies—which can be used to accurately predict flow-induced stresses in ICM.

After the specified melt volume is injected into the cavity during injection molding (IM) and ICM processes, the injection machine switches to either a post-filling (for IM) or a compression (for ICM) mode. In the post-filling stage for IM, the melt is continuously pushed into the cavity space to compensate for shrinkage from the gate. The flow-induced stresses therefore continue to increase during this period. Conversely, during the compression stage of ICM, the empty remaining section of the cavity is filled from the already-filled region. This means that the flow length is shorter in ICM than in IM. In addition, the molecule orientations are reconstructed because of the change in flow direction during the compression period. In most previous studies,[?,?,?] ICM flow variables (e.g., velocity and pressure) are first determined with the use of a fixed mesh. The velocity is then used to update the mesh location for the ICM simulations. Mesh motion, however, can influence the flow variables (e.g., convection), and this effect becomes apparent in the second step of the standard calculations.

To overcome this limitation, we have introduced a new material derivative to modify the governing and constitutive equations.[?] We have thus established a theoretical model with which we can effectively describe and predict compression flow during ICM. To that end, our model is expressed in terms of a 3D compressible and viscoelastic fluid and our material derivative includes the velocity of the mesh movement.

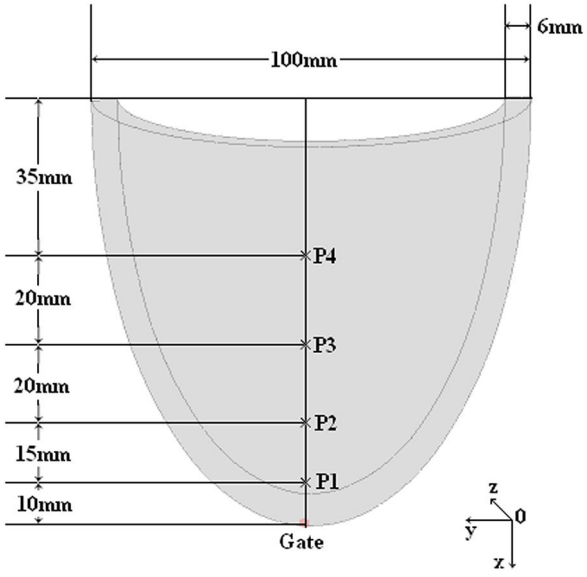

Figure 1. *Schematic diagram of the simulated part, showing its dimensions and the locations of the investigated points (P1–P4).*

In our methodology we use the arbitrary Lagrangian-Eulerian technique[?] to determine the filled region and update the flow field in the compression stage. We then use a finite element method (the eXtended Pom-Pom model) and an iterative approach to solve the flow problem and to simulate the evolution of the flow-induced stress. Based on our proposed theory and algorithm, we have also developed programming codes that are necessary to simulate the evolution of pressure, velocity, temperature, and stress during ICM.

Continued on next page

In the final part of our work, we conducted a simulation for a quarter of a spherical part with equal thickness (see Figure 1) to evaluate our proposed method. We investigated the flow-induced stresses—at four different points (P1–P4) on this part—that arise during both IM and ICM processes. Our results indicate that all the final flow-induced stresses are greater for IM than for ICM. For example, the maximum flow-induced stress (the zz component) at P1 is 10722.8Pa for IM and about three times less (3509.9Pa) for ICM (see Figure 2).

Our simulations also show that the evolution of the flow-induced stress in the gapwise direction (i.e., in the direction of P1–P4) is different for IM and ICM. We find that—for IM—the zz component of the flow-induced stress decreases as the distance to the gate increases (see Figure 3). This is the case during all the stages of the IM process. In contrast, our results indicate that the stress at P4 (i.e., farthest from the gate) exceeds the stress values at P2 and P3 (i.e., closer to the gate) at the end of the ICM compression stage (see Figure 4). Moreover, the corresponding residual stress (at the end of cooling) is greater at P4 than at either P2 or P3. P4 is at the far end of the cavity (i.e., it

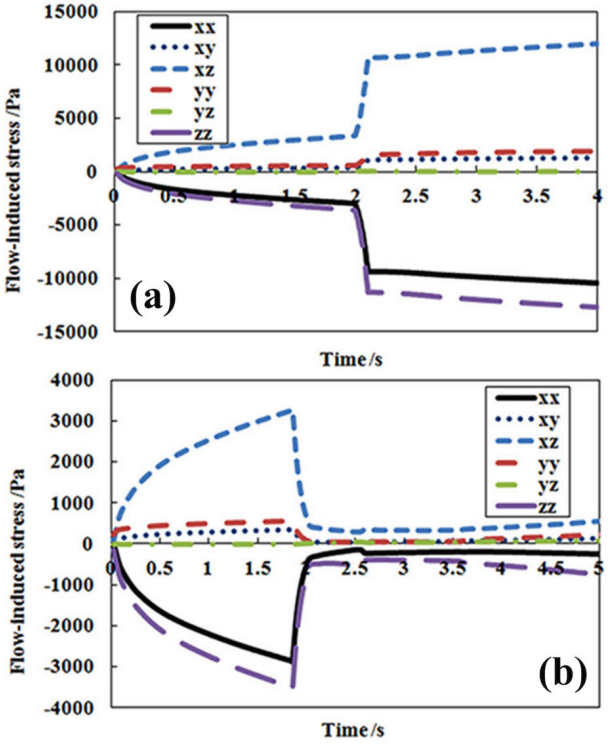

Figure 2. *Comparison of the flow-induced stress evolution at the near-gate position (P1) of the simulated part during (a) injection molding (IM) and (b) injection/compression molding (ICM). Each of the different directional components of the flow-induced stresses (i.e., xx, xy, xz, yy, yz, and zz) is shown.*

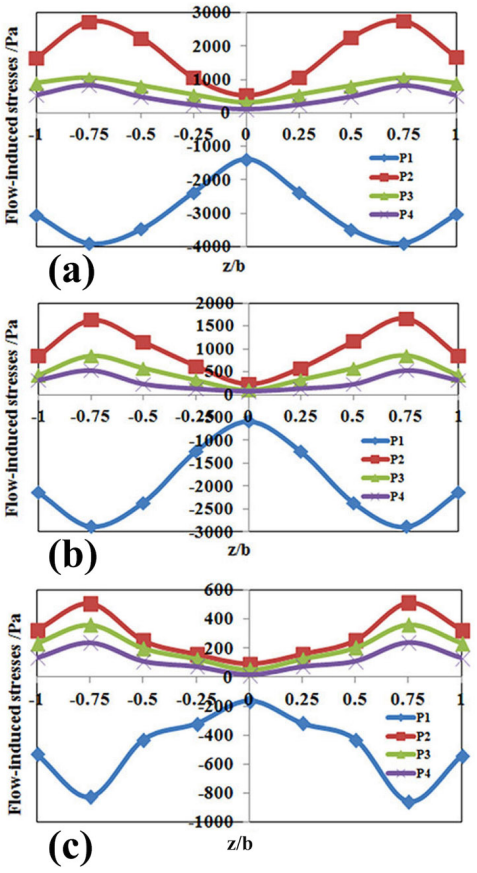

Figure 3. *Predicted flow-induced stress distributions (zz component) along the gapwise direction (i.e., at P1–P4) of the molded part during IM. The stress distributions are shown at three different times, i.e., at (a) the end of the filling process (1.8s), (b) the end of the packing process (17.3s), and (c) the end of the cooling process (47.3s). z/b: Normalized thickness, where z is the distance to the central plane and b is the half-thickness.*

is filled relatively late). The velocity at this point (near the flow end) therefore increases rapidly during compression, as has previously been demonstrated.[?] The flow-induced stress near the flow end is thus larger than at the other regions of the part during compression, and the residual flow-induced stresses we obtain for IM are almost twice the ICM values.

In summary, we have developed a new numerical approach to predict flow-induced stresses during ICM processes. Our method involves a twofold iteration, and we propose that it can be used to decouple the interdependence of velocity, stress, and temperature parameters during

Continued on next page

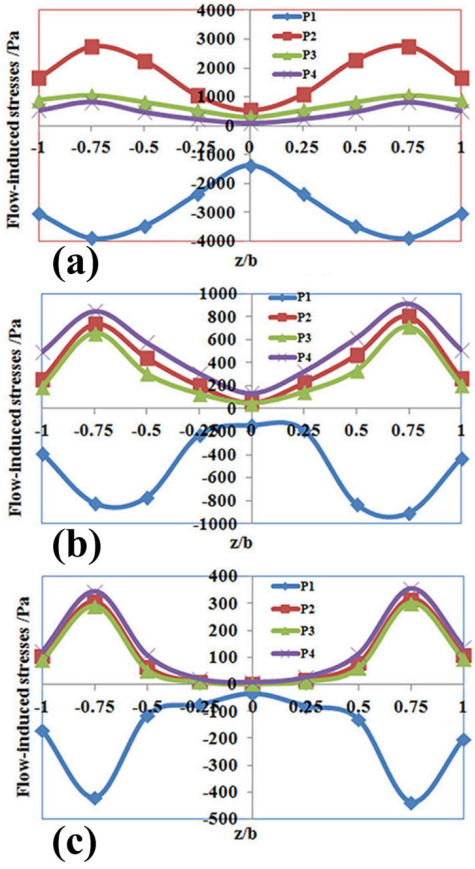

Figure 4. *Predicted flow-induced stress distributions (zz component) along the gapwise direction (i.e., at P1–P4) of the molded part during ICM at (a) the end of filling (1.8s), (b) the end of compression (52.3s), and (c) the end of cooling (82.3s).*

ICM modeling. With our methodology we can also overcome problems associated with the standard integral method (i.e., which requires a large amount of computational power and memory). The results of our simulations indicate that the flow-induced stress levels are significantly lower with ICM than with IM. In addition, higher compression velocities induce larger flow-induced stresses, increased melt temperatures cause decreased flow-induced stresses, and flow-induced stress is most significant in the regions of the flow start and end. In our future work we will focus on constructing a new constitutive model, which involves molecular orientation and a shear rate derivative, to improve the precision of our predictions.

Author Information

Wei Cao, Qian Zhang, Yanhui Qi, Guixiang Lu, and Changyu Shen
Zhengzhou University
Zhengzhou, China

References

1. M. Sortino, G. Totis, and E. Kuljanic, *Comparison of injection molding technologies for the production of micro-optical devices*, **Proc. Eng. 69**, pp. 1296–1305, 2014.
2. I. H. Kim, S. J. Park, S. T. Chung, and T. H. Kwon, *Numerical modeling of injection/compression molding for center-gated disk: part II. Effect of compression stage*, **Polym. Eng. Sci. 39**, pp. 1943–1951, 1999.
3. Y. B. Lee, T. H. Kwon, and K. Yoon, *Numerical prediction of residual stresses and birefringence in injection/compression molded center-gated disk. Part I: basic modeling and results for injection molding*, **Polym. Eng. Sci. 42**, pp. 2246–2272, 2002.
4. N. H. Kim and A. I. Isayev, *Birefringence in injection-compression molding of amorphous polymers: simulation and experiment*, **Polym. Eng. Sci. 53**, pp. 1786–1808, 2013.
5. W. Cao, Z. Min, S. Zhang, T. Wang, J. Jiang, H. Li, Y. Wang, and C. Shen, *Numerical simulation for flow-induced stress in injection/compression molding*, **Polym. Eng. Sci. 56**, pp. 287–298, 2016.
6. J.-Y. Ho, J. M. Park, T. G. Kang, and S. J. Park, *Three-dimensional numerical analysis of injection-compression molding process*, **Polym. Eng. Sci. 52**, pp. 901–911, 2012.
7. S.-C. Chen, Y.-C. Chen, H.-S. Peng, and L.-T. Huang, *Simulation of injection-compression molding process, part 3: effect of process conditions on part birefringence*, **Adv. Polym. Technol. 21**, pp. 177–187, 2002.